Miyahara *et al.*
Biotechnology for Sustainable Materials (2024) 1:7
https://doi.org/10.1186/s44316-024-00008-9

Biotechnology for Sustainable Materials

RESEARCH

Open Access

Biosynthesis of polyhydroxyalkanoate copolymers consisting of α-methylated monomer units from glucose and propionate: thermal properties and chiral configuration

Yuki Miyahara[1*], Marii Ishino[1], Christopher T. Nomura[2], Seiichi Taguchi[3], Hideki Abe[4] and Takeharu Tsuge[1*]

Abstract

Background Expression of the *Ascaris suum* ketothiolase (Acat3) in recombinant *Escherichia coli* enables the production of α-methylated monomers such as 3-hydroxy-2-methylvalerate (3H2MV) and 3-hydroxy-2-methylbutyrate (3H2MB) for polyhydroxyalkanoate (PHA) biosynthesis from glucose and propionate as carbon sources. However, the chiral configurations and thermal properties of biosynthesized PHAs remain poorly understood.

Results In this study, 3-hydroxybutyrate (3HB)-based PHA copolymers containing 3H2MV and 3H2MB units were synthesized from glucose and propionate using Acat3-expressing *Escherichia coli* LSBJ. The 3H2MV fraction of the synthesized PHA reached 15.7 mol%, while the 3H2MB fraction remained at approximately 0.2 mol%. Chirality analysis revealed that (2*S*,3*R*)- and (2*R*,3*R*)-3H2MV units were both detected; however, (2*R*,3*R*)-3H2MV units were dominant in the PHA copolymer produced by the strain expressing the (*R*)-specific enoyl-CoA hydratase ($PhaJ_{Ac}$). To evaluate the effect of α-methylated monomers on the crystallization behavior of PHA copolymers, cold crystallization was compared for PHA polymers with different mol% 3-hydroxyvalerate (3HV) monomer units. The cold crystallization of the copolymer containing 11 mol% 3H2MV and 30 mol% 3HV was detected at 68 °C, while the non-α-methylated copolymer containing 24 mol% 3HV did not exhibit cold crystallization, indicating that α-methylated PHA had a greater tendency to crystallize.

Conclusions This study conclusively demonstrated that (2*S*,3*R*)- and (2*R*,3*R*)-3H2MV units were both incorporated into PHA by expressing Acat3; however, the (2*R*,3*R*)-isomer became the dominant 3H2MV unit in the PHA copolymers by additionally expressing $PhaJ_{Ac}$. The 3H2MV repeating unit facilitated the crystallization of PHA copolymers despite the high fraction of the 3HV unit.

Keywords Polyhydroxyalkanoate, PHA, α-methylated monomer, 3-hydroxy-2-methylvalerate, 3H2MV, Crystallization, Chiral configuration

*Correspondence:
Yuki Miyahara
miyahara.y.aa@m.titech.ac.jp
Takeharu Tsuge
tsuge.t.aa@m.titech.ac.jp
Full list of author information is available at the end of the article

Graphical Abstract

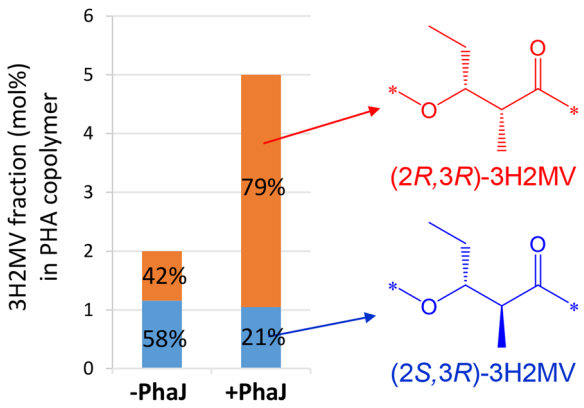

Introduction

Polyhydroxyalkanoates (PHAs) are environmentally friendly bioplastics naturally biosynthesized by microorganisms for intracellular carbon storage [1–3]. PHAs have exhibited excellent biodegradability in various environments including compost, soil, river water, and seawater [4, 5]. The most representative PHA, poly[(*R*)-3-hydroxybutyrate] [P(3HB) or PHB], is brittle and inflexible owing to its high degree of crystallinity [1]. Therefore, 3HB-based PHA copolymers have been developed to improve material properties by reducing the degree of crystallinity [6]. Some of the most common variations of PHA monomers used to alter the material properties of 3HB-based copolymers are shown in Fig. 1.

Among these, the copolymer of 3HB and (*R*)-3-hydroxyhexanoate (3HHx) [P(3HB-*co*-3HHx)] exhibits good flexibility and ductility, making it an incredibly useful PHA. Thus, the copolymerization of distinct comonomers is considered beneficial for improving the mechanical properties of PHAs [7, 8]. A high degree of crystallinity may hamper some physical properties of polymers, while slow crystallization is a drawback for plastic processing. Copolymerizing 3HB with representative comonomers such as (*R*)-3-hydroxyvalerate (3HV) and 3HHx leads to a slow copolymer crystallization rate, thereby reducing the efficiency of the melt molding process [6, 9–11]. Hence, the development of PHA copolymers with rapid crystallization behavior is desired. Recently, PHAs consisting of α-methylated monomers such as 3-hydroxy-2-methylbutyrate (3H2MB) and 3-hydroxy-2-methylvalerate (3H2MV) have been biosynthesized by recombinant *Escherichia coli* using an artificial metabolic pathway from *trans*-2-methyl-2-butenate (tiglic acid) and *trans*-2-methyl-2-pentenoic acid as precursors [12–18]. These studies indicate that PHAs containing α-methylated monomers exhibit rapid crystallization behaviors distinct from those of P(3HB) and conventional 3HB-based copolymers. In particular,

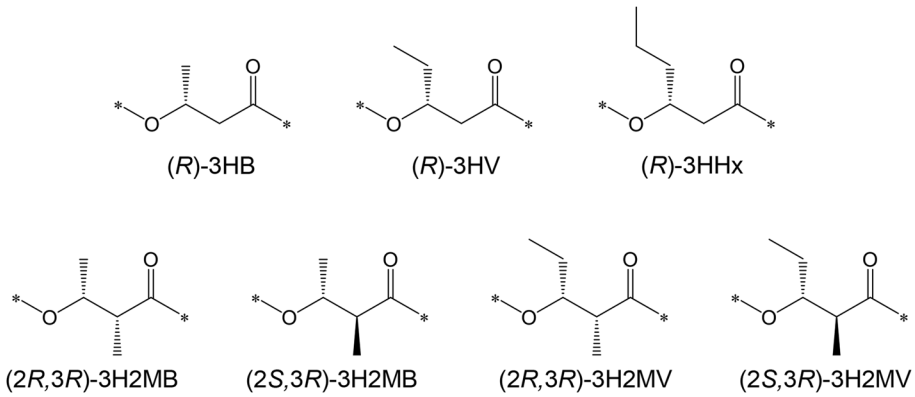

Fig. 1 Chemical structures of various PHA monomers

P(3H2MB) exhibits ~ 200-fold faster primary nucleation rate compared with that of P(3HB) [16]. Previously, the crystallization rates of P(3HB-*co*-11 mol% 3H2MV) [PHBM11], in which 3H2MV has a methyl side chain at the α-position of 3HV backbone, and P(3HB-*co*-12 mol% 3HV) [PHBV12] were evaluated by measurement of half-crystallization time ($t_{1/2}$). The $t_{1/2}$ of PHBM11 at a 75 °C isothermal crystallization temperature was 1.56 min [18], whereas the $t_{1/2}$ of PHBV12 at 80 °C was as long as 39.05 min [11]. Thus, α-methylated monomers confer superior crystallization behavior compared to typical (*R*)-3-hydroxyalkanoate monomers in PHA copolymers, which would lead to greater processability [16, 18]. Therefore, PHAs containing α-methylated monomer units have exciting potential as novel bio-based and biodegradable plastic materials.

The chirality of the α-carbon of monomers influences PHA's thermal and mechanical properties. Indeed, it has been reported that for PHAs containing 3-hydroxy-2-methylpropionate (3H2MP), a new type of α-methylated monomer, the mechanical properties of the PHA differ dependent on the stereoisomeric configuration at the α-carbon [19]. The *S*-configuration at the β-position of the monomers cannot be polymerized by PHA synthase, but both *S*- and *R*-configurations at the α-position of these monomers are available [19]. The stereoisomeric composition at the α-position in the monomers can be used to control the physical properties of PHA.

Ketothiolase (Acat3) from *Ascaris suum* catalyzes Claisen condensation reactions and enables the coupling of acetyl-CoA and propionyl-CoA. This produces four kinds of 3-oxoacyl-CoAs: 3-oxobutyryl-CoA, 3-oxovaleryl-CoA, 3-oxo-2-methylbutyryl-CoA, and 3-oxo-2-methylvaleryl-CoA, dependent on the substrate access to the active site of Acat3 [20] (Fig. 2).

Dong et al. [21] constructed recombinant *E. coli* expressing Acat3, acetoacetyl-CoA reductase (PhaB), and PHA synthase, and were able to produce PHA copolymers containing up to 36 mol% of α-methylated monomers (3H2MB and 3H2MV units) from glucose and propionate. Nevertheless, the effect of introducing α-methylated monomers into PHA copolymers on the resulting thermal properties, as well as the stereoisomeric configuration at the α-position of α-methylated monomers synthesized using Acat3, remains to be elucidated.

In this study, PHA copolymers with α-methylated monomers were biosynthesized from glucose and propionate by recombinant *E. coli* LSBJ, which expresses Acat3 to construct an artificial metabolic pathway. Subsequently, the stereochemical configuration at the α-position in the biosynthesized PHA copolymers was determined. Finally, the effect of α-methylated monomers on the thermal properties of PHA copolymers was elucidated.

Materials and methods

Materials

Methyl (2*S*,3*R*)-3H2MV was purchased from Enamine Ltd. (Kyiv, Ukraine) and used as a standard for gas

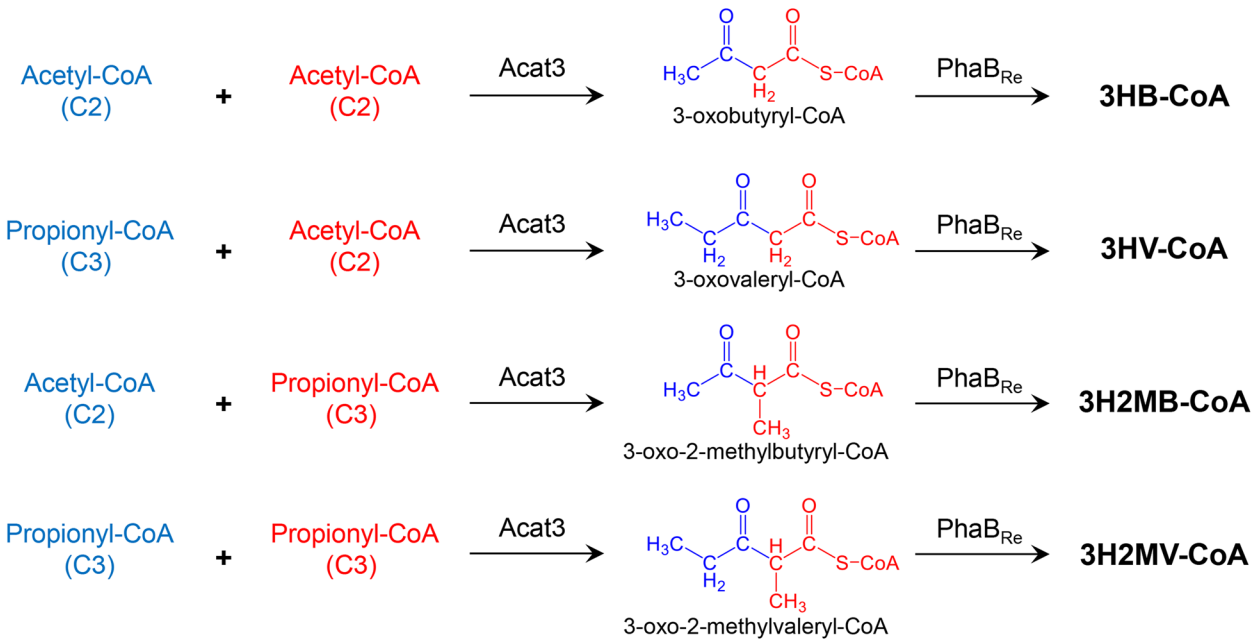

Fig. 2 PHA monomers biosynthesis pathway by ketothiolase (Acat3) and NADPH-dependent acetoacetyl-CoA reductase ($PhaB_{Re}$)

chromatography–mass spectrometry (GC–MS) analysis. P(3HB) [PHB] and P(3HB-*co*-24 mol% 3HV) [PHBV24] were provided by Monsanto Co., Ltd. (Creve Coeur, MO, USA) and Sigma-Aldrich (St. Louis, MO, USA), respectively. P(3HB-*co*-11 mol% 3H2MV) [PHBM11] was synthesized in our previous study [18].

Bacterial strains and plasmids

The bacterial strains and plasmids used in this study are listed in Table S1. *Escherichia coli* LSBJ [22, 23], an engineered strain of *E. coli* LS5218 [*fadR601*, *atoC(Con)*] with *fadB* and *fadJ* double deletions, was used as the host strain for PHA biosynthesis. The recombinant plasmid pBBR1*phaP*(D4N)$C_{NSDG}J_{Ac}$_*acat3-phaB*, carrying the PHA synthase ($PhaC_{Ac}$_NSDG mutant) gene, PHA granule-associated protein ($PhaP_{Ac}$ D4N mutant) gene, (*R*)-specific enoyl-CoA hydratase ($PhaJ_{Ac}$) gene from *Aeromonas caviae* FA440, acetoacetyl-CoA reductase ($PhaB_{Re}$) gene from *Ralstonia eutropha* H16, and ketothiolase (Acat3) gene from *A. suum*, was transformed into *E. coli* LSBJ. The plasmid pBBR1*phaP*(D4N)C_{NSDG}_*acat3-phaB*, constructed by removing $phaJ_{Ac}$ gene from pBBR1*phaP*(D4N)$C_{NSDG}J_{Ac}$_*acat3-phaB*, was used to study the effects of $PhaJ_{Ac}$ expression on PHA biosynthesis. To increase the supply of propionyl-CoA in the cytosol, the propionyl-CoA transferase genes from *Megasphaera elsdenii* (pct_{Me}) and *R. eutropha* H16 (pct_{Re}) were expressed using pTTQ19-pct_{Me} and pTTQ19-pct_{Re}, respectively (Table S1) [13, 14].

Plasmid construction

The construction strategy for the plasmid vectors is illustrated in Supplemental Figure S1. To introduce the *acat3* gene in pBBR1*phaP*(D4N)$CJ_{Ac}AB_{Re}$NSDG [12], the plasmid was digested by *Spe*I and *Bam*HI. Subsequently, the pha_{Re} promoter of *R. eutropha* H16 was amplified by polymerase chain reaction (PCR) using the following primers: BamH1-Pre-F, 5'-AAAGGATCCCGGGGCAAG TACCTT-3'; Pre-Spe1-R, 5'-AAAACTAGTCCGGCT CCGGGCATTG-3' (Table S1). The resulting amplified fragment (approximately 1 kb) was inserted into the *Spe*I and *Bam*HI sites of pBBR1*phaP*(D4N)$CJ_{Ac}AB_{Re}$NSDG to yield pBBR1*phaP*(D4N)CJ_{Ac} NSDG_P_{Re}. Next, $phaB_{Re}$ with the Shine–Dalgarno (SD) sequence from the pET3a vector was amplified from pET3a::*phaB* [24] using the primer sets (pET3a-aaa-xba1-F and aaaSac2-phaB-R). The *acat3* (GenBank, ADY44833.1) was chemically synthesized by Eurofins Genomics Co. Ltd. (Tokyo, Japan) based on the sequence of *A. suum* (Table S1), and its codon usage was optimized for *E. coli*. The $phaB_{Re}$ and *acat3* genes were introduced into the *Xba*I-*Sac*II and *Spe*I-*Xba*I sites of pBBR1*phaP*(D4N)CJ_{Ac} NSDG_P_{Re}, respectively, then pBBR1*phaP*(D4N)$C_{NSDG}J_{Ac}$_*acat3-phaB* was obtained.

To construct a $phaJ_{Ac}$-deficient plasmid vector, the 2.7 kb DNA fragment of pha_{Re} promoter-*phaP*(D4N)-$phaC_{NSDG}$ was amplified by overlap PCR using follows primer sets: PacNSDG_infusion -F1, 5'-TCGACGGTA GCTTGATATCCGATCTGGACCGGGGT-3'; PacNSDG_ infusion -R1, 5'-CATCATCGGTCTCCGAATTCAGTT CGGCAGAACAG-3'; PacNSDG_infusion -F2, 5'-CTG TTCTGCCGAACTGAATTCGGAGACCGATGATG-3'; PacNSDG_infusion -R2, 5'-CCCGGGCTGCAGGAA TTCTCATGCGGCGTCCTCCT-3'. Subsequently, the resultant PCR fragment was integrated into the *Eco*RV and *Eco*RI sites of the pBBR1*phaP*(D4N)$C_{NSDG}J_{Ac}$_ *acat3-phaB* vector using an In-Fusion HD Cloning Kit (Takara Bio Inc., Ohtsu, Japan). Finally, the pBBR1*phaP* (D4N)C_{NSDG}_*acat3-phaB* was constructed.

The pct_{Re} gene was amplified from the genomic DNA of *R. eutropha* H16 using following primers: Nde1_PCT-Re, 5'-ATACATATGAAGGTGATCACCGCACGCGAA GCGG-3'; PCT-Re_BamH1, 5'-GCCGGATCCTTACAG GTGCAGGGGCCCGG-3'(See Table S1). The amplified DNA fragment (1.6 kb) was inserted into the *Nde*I and *Bam*HI site of the pET3a vector to yield the pET3a_ PCT_{Re}. Next, pET3a_PCT_{Re} was digested by *Xba*I and *Bam*HI restriction enzymes to obtain the DNA fragment containing pct_{Re} gene with the SD sequence from the pET3a vector. Subsequently, the *SD*-pct_{Re} gene fragment was inserted into the pTTQ19 vector, to yield pTTQ19_pct_{Re}.

PHA biosynthesis

The recombinant *E. coli* was freshly transformed for each experiment and then pre-cultivated in Luria–Bertani (LB) medium (10 g/L NaCl, 10 g/L Bacto-tryptone, 5 g/L Bacto-yeast extract) supplemented with 50 mg/L of kanamycin (Km) and 50 mg/L of carbenicillin (Cb) at 30 °C for 15 h. For PHA biosynthesis, 5% (v/v) of seed culture was inoculated into a 500 mL shake flask containing 100 mL (final volume) of the culture medium and cultivated at 30 °C for 76 h. The 50 mg/L of antibiotics (Km and Cb) and 1 mM isopropyl-β-D-thiogalactopyranoside (IPTG) were added to the culture medium for plasmid maintenance and to induce *pct* expression. Glucose (20 g/L) and sodium propionate (3 or 9 g/L) were added at the beginning of cultivation and after 4 h of culture, respectively. The M9 mineral medium employed in this study was composed of the following: 17.1 g/L $Na_2HPO_4{\cdot}12H_2O$, 3 g/L KH_2PO_4, 1 g/L NH_4Cl, 0.5 g/L NaCl, 2 mL of 1 M $MgSO_4{\cdot}7H_2O$, 0.1 mL of 1 M $CaCl_2$.

PHA quantification

PHA accumulation in cells was determined by gas chromatography (GC) using a Shimadzu GC-2014s (Shimadzu, Kyoto, Japan) equipped with an Inert Cap 1 (GL Sciences, Tokyo, Japan). Approximately 15–20 mg of lyophilized cells were treated with 2 mL chloroform and 2 mL of methanol/sulfuric acid (85:15 vol%) at 100 °C for 8 h to prepare the samples. The samples were then injected into the chromatograph. The heating program has been described previously [25].

PHA extraction and purification

Polymers were extracted from the lyophilized cells using chloroform at 60 °C for 1–3 h. The polymer solution was passed through filter paper No. 1 (ADVANTEC, Toyo Roshi Kaisha, Ltd., Tokyo, Japan) and precipitated in methanol to remove impurities such as culture components. The polymers were collected using No. 5B filter paper (ADVANTEC) and dried at room temperature. Solvent-cast films of the PHAs were prepared to analyze their thermal properties. For this purpose, the purified polymers were dissolved in chloroform and then filtered with a 0.45 μm polyvinylidene fluoride filter on a Petri dish and dried in a draft chamber. The cast film was aged at room temperature for 3–4 weeks to achieve consistent crystallization before analysis.

Polymer structural analysis

The microstructures and monomer compositions of the biosynthesized PHAs were analyzed by nuclear magnetic resonance (NMR) spectroscopy using an AVANCE III HD500 spectrometer (Bruker BioSpin GmbH, Ettlingen, Germany). Approximately 5–20 mg of the purified polymers were dissolved in 1 mL of $CDCl_3$ and subjected to 500 MHz ^{1}H NMR and 125 MHz ^{13}C NMR spectroscopic analyses. The monomer composition was determined by calculating the ratio of peak areas in the NMR spectra.

Chirality analysis

The chiral configurations of the biosynthesized PHAs were determined by gas chromatography–mass spectrometry (GC-MS; QP2010, Shimadzu, Kyoto, Japan) equipped with a Beta-DEX 120 column (Supelco, Bellefonte, PA, USA). The column temperature was initially set at 100 °C, increased to 140 °C at a rate of 5 °C/min, and further increased to 200 °C at a rate of 10 °C/min. The mass spectrum was set *m/z* 88 based on the fragmentation pattern of the methyl ester of α-methylated monomers. The stereoisomeric molar ratios were determined by calculating the peak area of each isomer at *m/z* 88.

Thermal property analysis

The melting and crystallization behaviors of the polymer samples were analyzed using differential scanning calorimetry (DSC) (DSC 8500, PerkinElmer, Waltham, MA, USA) under a helium atmosphere. Approximately 5 mg of each polymer sample was weighed and sealed in an aluminum pan. First, the temperature was maintained for 2 min at -50 °C, followed by increasing to 200 °C at 20 °C/min (first heating scan) and holding at 200 °C for 1 min. Subsequently, the temperature was rapidly decreased to -50 °C at a cooling rate of 500 °C/min, held for 2 min, then increased again to 200 °C (second heating scan), and held for 2 min. Next, the temperature was decreased to -50 °C at a cooling rate of 20 °C/min (cooling scan). The original melting temperature (T_m) and enthalpy of fusion (ΔH_m) were determined from the first heating scan, whereas the glass transition (T_g) and cold crystallization (T_{cc}) temperatures were determined from the second heating scan. The crystallization temperature (T_c) was determined using cooling scans.

Results

Effect of $PhaJ_{Ac}$ expression on PHA biosynthesis

The α-methylated 3H2MB and 3H2MV units are generated by Acat3 via Claisen condensation reactions of propionyl-CoA with acetyl-CoA and propionyl-CoA, respectively (Fig. 2). Therefore, propionate is required as a precursor for α-methylated monomers. Furthermore, 3-oxoacyl-CoA, synthesized via the condensation reaction catalyzed by Acat3, may be converted into enoyl-CoA by the action of $PhaB_{Re}$ and an inherent dehydratase in *E. coli* (Fig. 3). The (*R*)-specific enoyl-CoA hydratase ($PhaJ_{Ac}$) catalyzes the hydroxylation reaction at the β-position of enoyl-CoA, an intermediate in the fatty acid β-oxidation, leading to the formation of (*R*)-3-hydroxyacyl-CoA. Therefore, introducing $PhaJ_{Ac}$ in the Acat3-expressing strain might affect the production of α-methylated monomers.

Given the potential roles of Acat3 and $PhaJ_{Ac}$ on the production of α-methylated PHA polymers, we desired to characterize the effect of propionate concentration and $PhaJ_{Ac}$ expression on PHA biosynthesis using recombinant *E. coli* LSBJ expressing $phaP_{Ac}$*_D4N*, $phaC_{Ac}$*_NSDG*, $phaJ_{Ac}$, *acat3*, $phaB_{Re}$, and pct_{Me} and compare the production and polymer composition with a strain in the absence of $phaJ_{Ac}$. The results are shown in Fig. 4.

PHA production by the $PhaJ_{Ac}$-expressing strain was comparable to that by the non-$PhaJ_{Ac}$-expressing strain. In the non-$phaJ_{Ac}$-expression strain, the α-methylated monomers fraction increased with the addition of sodium propionate, reaching a maximum of 2.4 mol% of 3H2MV unit at the supplementation of

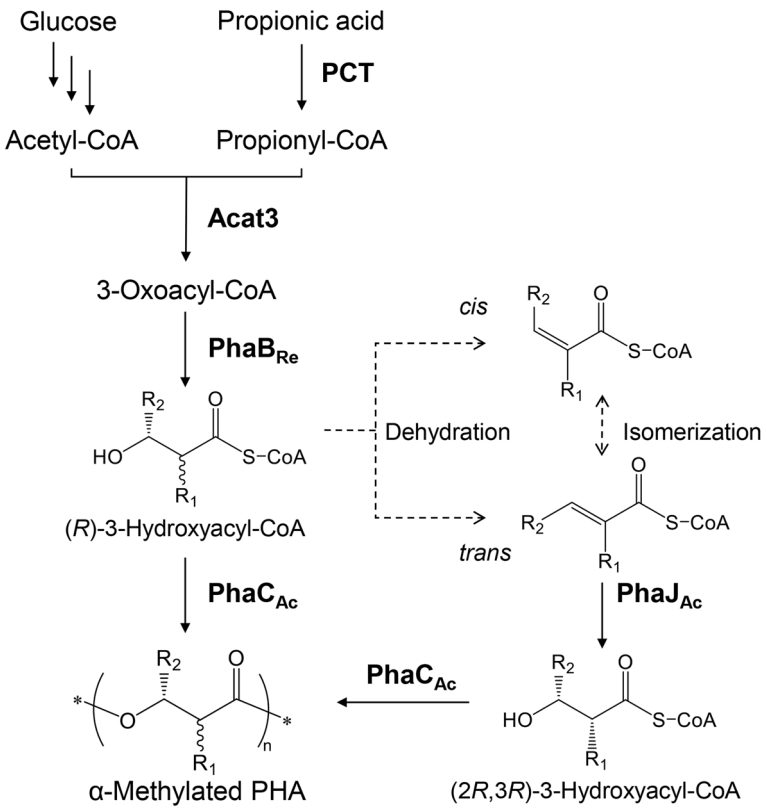

Fig. 3 The proposed metabolic pathway for α-methylated PHA generation via dehydration and hydration reactions, catalyzed by an inherent dehydratase and heterologously expressed (*R*)-specific hydratase (PhaJ$_{Ac}$). R$_1$: proton or methyl group, R$_2$: methyl or ethyl group

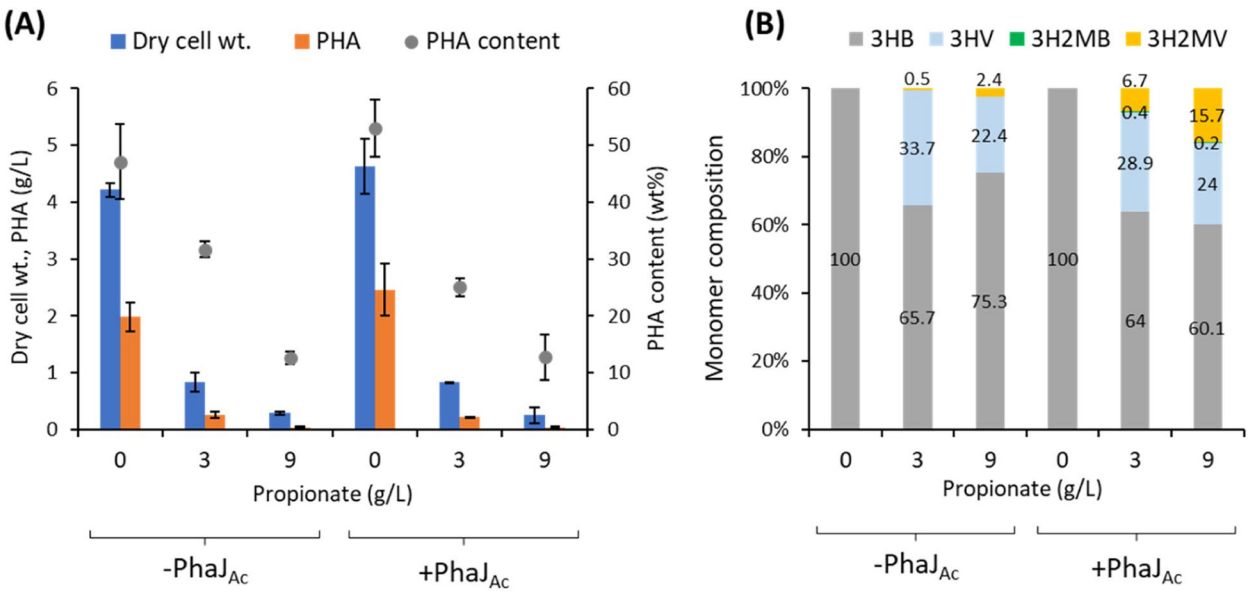

Fig. 4 PHA accumulation in the recombinant *E. coli* LSBJ with or without PhaJ$_{Ac}$ expression. **A** Dry cell weight, PHA concentration, and PHA content in the cells, **B** monomer composition of PHA determined by GC. The cells were cultivated in 100 mL M9 mineral medium supplemented with glucose (20 g/L, added at 0 h) and sodium propionate (3 or 9 g/L, added at 4 h) at 30 °C for 76 h. All experiments were repeated at least three times. Non-PhaJ$_{Ac}$ expression (-PhaJ$_{Ac}$): *E. coli* LSBJ/pTTQ19_*pct*$_{Me}$, pBBR1*phaP*(D4N)*C*$_{NSDG}$_*acat3-phaB*, PhaJ$_{Ac}$ expression (+PhaJ$_{Ac}$): *E. coli* LSBJ/pTTQ19_*pct*$_{Me}$, pBBR1*phaP*(D4N)*C*$_{NSDG}$*J*$_{Ac}$_*acat3-phaB*

9 g/L propionate. However, the fraction of α-methylated monomers in the $PhaJ_{Ac}$-expressing strain was reached at 15.9 mol% (3H2MV 15.7 mol%, 3H2MB 0.2 mol%) under the condition supplementing 9 g/L sodium propionate, which is 6.6-fold higher than that of the non-$PhaJ_{Ac}$-expressing strain. Despite the increases in 3H2MV monomer content in PHA copolymer produced with increasing amounts of propionate feedstock, those same increases inhibited PHA accumulation and cell growth (Fig. 4A). The 3H2MB fraction was detected in insignificant amounts; thus, it was ignored in subsequent analyses.

PHA biosynthesis and sample preparation

To prepare the polymer samples for characterization, repeated and scaled-up cultures were performed under the conditions shown in Table 1.

In these cultures, 3–15 g/L propionate was added to increase the diversity of 3H2MV unit composition in PHA copolymers. Furthermore, the sequential addition of glucose was performed to enhance PHA production. New PCT, an enzyme derived from *R. eutropha* H16, was also assessed. Biosynthesized PHAs were purified, and the PHA yields ranged from 13–196 mg. The highest molecular weight of PHA was observed for the non-$PhaJ_{Ac}$-expressing strain, with an M_w of 27.9×10^5 g/mol (Table 2). The polydispersity (M_w/M_n) of these polymers ranged from 1.57–2.60.

NMR analysis of biosynthesized PHA

The chemical structures of the biosynthesized PHA were analyzed using NMR. Figure 5 shows a 500 MHz ^{1}H NMR spectrum and a 125 MHz ^{13}C NMR spectrum with assigned proton and ^{13}C resonances, respectively. Signals

Table 1 Culture conditions for PHA sample preparation and monomer composition of prepared samples

Culture condition					Polymer yield (mg)[b]	Monomer composition (mol%)[c]			3H2MV isomer (%)[d]		Sample code
$PhaJ_{Ac}$	PCT[a]	Propionate (g/L)	Glucose (g/L) × times	Culture vol. (mL) × times		3HB	3HV	3H2MV	*2R*	*2S*	
+	Me	3	20 × 1	100 × 10	87	66	32	3	47	53	V32M3
-	Me	9	20 × 1	1000 × 3	196	63	35	2	42	58	V35M2-J
+	Me	9	20 × 1	1000 × 3	13	73	22	5	79	21	V22M5
+	Me	15	10 × 3	1000 × 4	112	59	30	11	79	21	V30M11
+	Re	15	10 × 3	100 × 10	21	82	14	4	82	18	V14M4

The cells were cultivated in 500 mL- or 2 L-shake flask containing M9 mineral medium supplemented with glucose (20 g/L added at 0 h or 10 g/L added at 0, 24, 48 h three times) and sodium propionate (3, 9, or 15 g/L, added at 4 h) at 30 °C for 76 h

[a] Propionyl-CoA transferase (PCT) from *Megasphaera elsdenii* (Me) or *Ralstonia eutropha* H16 (Re)

[b] Yield of purified polymer

[c] Copolymer compositions were determined using ^{1}H NMR (3H2MB unit was ignored)

[d] Isomeric ratios of 2*R* (%) and 2*S* (%) were calculated using the peak area detected by GC–MS equipped with a chiral separation column

Table 2 Thermal properties, molecular weight, and monomer sequence distribution (*D* value) of biosynthesized PHA copolymers

Sample code	1st heating		2nd heating		Cooling	Molecular weight		*D* value
	T_m (°C)	ΔH_m (J/g)	T_g (°C)	T_{cc} (°C)	T_c (°C)	M_w ($\times10^5$)	M_w/M_n	
PHB	161, 174	66	1	45	68	4.58	2.05	-
PHBV12	137, 150	28	-2	51	n.d	1.69	1.58	1.10
PHBV24	99	6	-10	n.d	n.d	0.47	1.71	1.07
V14M4	165, 176	47	-9, 1	58	57	8.03	2.37	13.8
V22M5	51, 162, 171	21	-10, 0	75	n.d	15.7	2.51	3.91
V30M11	50, 163, 174	23	-7, 1	68	n.d	8.24	2.60	2.19
V32M3	80, 166, 179	35	-13, 0	64	n.d	7.68	1.83	6.81
V35M2-J	73, 164, 172	27	-13, 0	74	n.d	27.9	1.57	4.84

DSC measurements were conducted at heating and cooling scan rates of 20°C/min

n.d. Not detectable

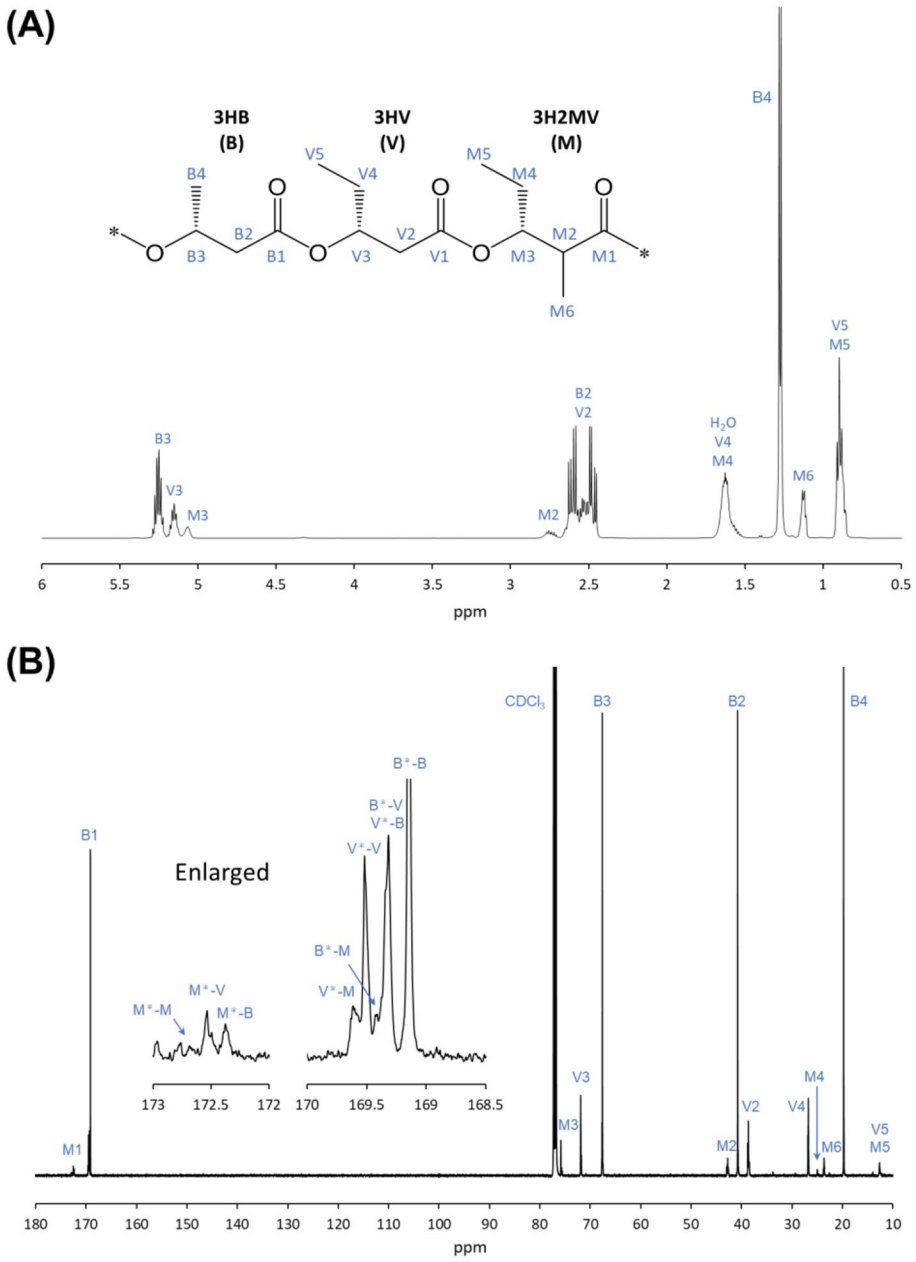

Fig. 5 **A** 500 MHz ^{1}H NMR and **B** 125 MHz ^{13}C NMR spectrum of biosynthesized PHA (sample V30M11)

of α-methyl protons (-CH_3) of 3H2MV (1.13 ppm) were detected in the ^{1}H NMR spectrum (Fig. 5A). Furthermore, signals corresponding to the β-methine carbon and β-methylene carbon of 3H2MV were observed at 75.8 ppm and 23.6 ppm in the ^{13}C NMR spectrum, respectively (Fig. 5B), confirming the inclusion of 3H2MV monomer in the biosynthesized PHA. Based on ^{1}H NMR analysis, the monomer composition of biosynthesized PHA was calculated to be 59 mol% 3HB, 30 mol% 3HV, and 11 mol% 3H2MV (sample V30M11).

Subsequently, the monomer sequence distribution was examined from the signals derived from the carbonyl carbons (169–173 ppm) to determine whether it was a statistically random copolymer. Based on the Bernoulli distribution, there are $F_{B\text{-}B}$, $F_{B\text{-}A}$, $F_{A\text{-}B}$, and $F_{A\text{-}A}$ (*B* and *A* represent the 3HB and other 3-hydroxyalkanoate units, respectively), where $F_{B\text{-}A}$ is the mole fraction of the *BA* distribution, and *D* is used to calculate the randomness of the copolymer, which is defined as follows [26]:

$$D = \frac{F_{B-B}F_{A-A}}{F_{B-A}F_{A-B}}$$

Theoretically, the D value of a statistically random copolymer should be equal to 1: Blocky copolymers have D values much higher than 1, whereas alternating copolymers have D values close to 0 [26].

The D values of the copolymer samples were calculated from the carbonyl peaks detected in the ^{13}C NMR spectrum (Fig. 5B). As shown in Table 2, the copolymers with D values of α-methylated PHA range from 2.19 to 13.8, suggesting their classification as slightly blocky copolymers. Indeed, when comparing the diad distributions of 3H2MV*-3HB (M*-B) and 3H2MV*-3HV (M*-V) observed at around 172.5 ppm in the ^{13}C NMR spectrum (Fig. 5B), M*-V signal is larger than M*-B signal, which differs from the abundance ratio of 3HB and 3HV units in the copolymer.

Chirality analysis of biosynthesized PHA

The biosynthesized α-methylated monomers possess chiral characteristics due to the chiral centers on their α-carbons. The methyl-esterified PHA monomers were analyzed using GC–MS with a chiral separation column. Chemically synthesized methyl (2*S*,3*R*)-3-hydroxy-2-methylvararate was used as a standard.

As shown in Fig. 6, by selecting the ion chromatogram of *m/z* 88 based on the fragmentation pattern of the methyl ester of α-methylated monomers, a clear separation was observed for the two stereoisomers with retention times of 5.2 and 5.4 min for methyl (2*R*)-isomer and methyl (2*S*)-isomer, respectively. The 3H2MV peak of the sample V35M2-J (produced by non-PhaJ$_{Ac}$-expressing strain) was detected at both 5.3 min and 5.4 min. Based on the peak areas, the *R: S* ratio was calculated as 42:58. Interestingly, the (2*R*)-isomer ratio increased in sample V22M5 (produced by PhaJ$_{Ac}$-expressing strain), resulting in a high (2*R*)-isomer ratio of 79%. PhaJ$_{Ac}$ expression enhanced the supply of (2*R*)-isomer. In our previous study [18], we synthesized PHBM11 by PhaJ$_{Ac}$-expressing recombinant *E. coli* LSBJ using *trans*-2-methyl-2-pentenoic acid as the 3H2MV precursor. PHBM11 was subjected to GC–MS analysis in this study. The result indicates that nearly all detectable 3H2MV units incorporated into PHA are (2*R*)-isomers (Fig. 6). This strongly suggests that PhaJ$_{Ac}$ hydroxylates carbon in a (2*R*)-specific manner to provide (*2R,3R*)-3H2MV units.

Thermal properties of biosynthesized PHA

Examination of the effect of incorporating α-methylated monomers into PHA polymers on their thermal properties was explored using DSC. The melting temperature

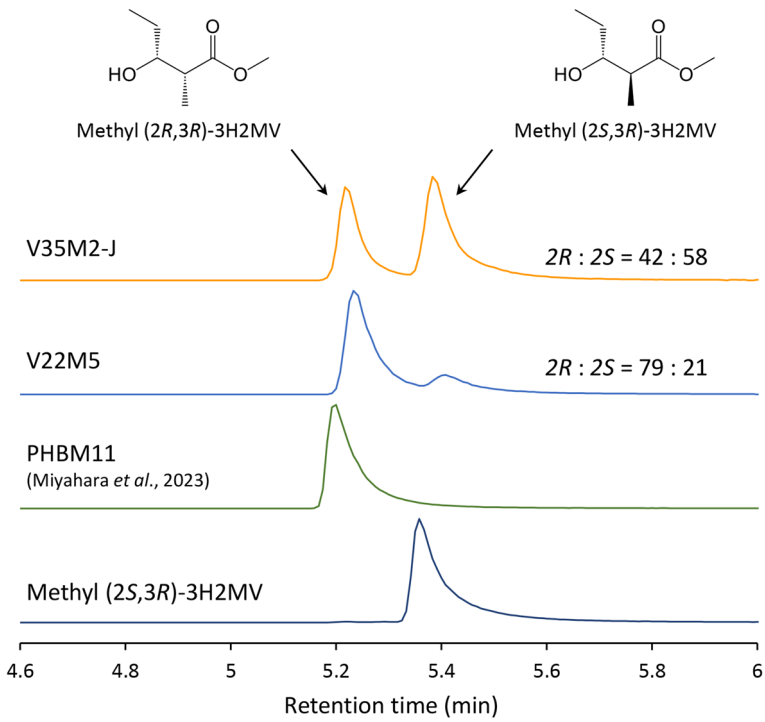

Fig. 6 Chiral configuration analysis of PHA methyl esters and methyl (2*S*,3*R*)-3H2MV by GC–MS equipped with a chiral separation column. The GC–MS ion chromatograms (*m/z* 88) are shown. PHA copolymer samples of V35M2-J and V22M5 were biosynthesized by non-PhaJ$_{Ac}$-expressing and PhaJ$_{Ac}$-expressing strains, respectively. PHBM11 were biosynthesized in our previous study [18]

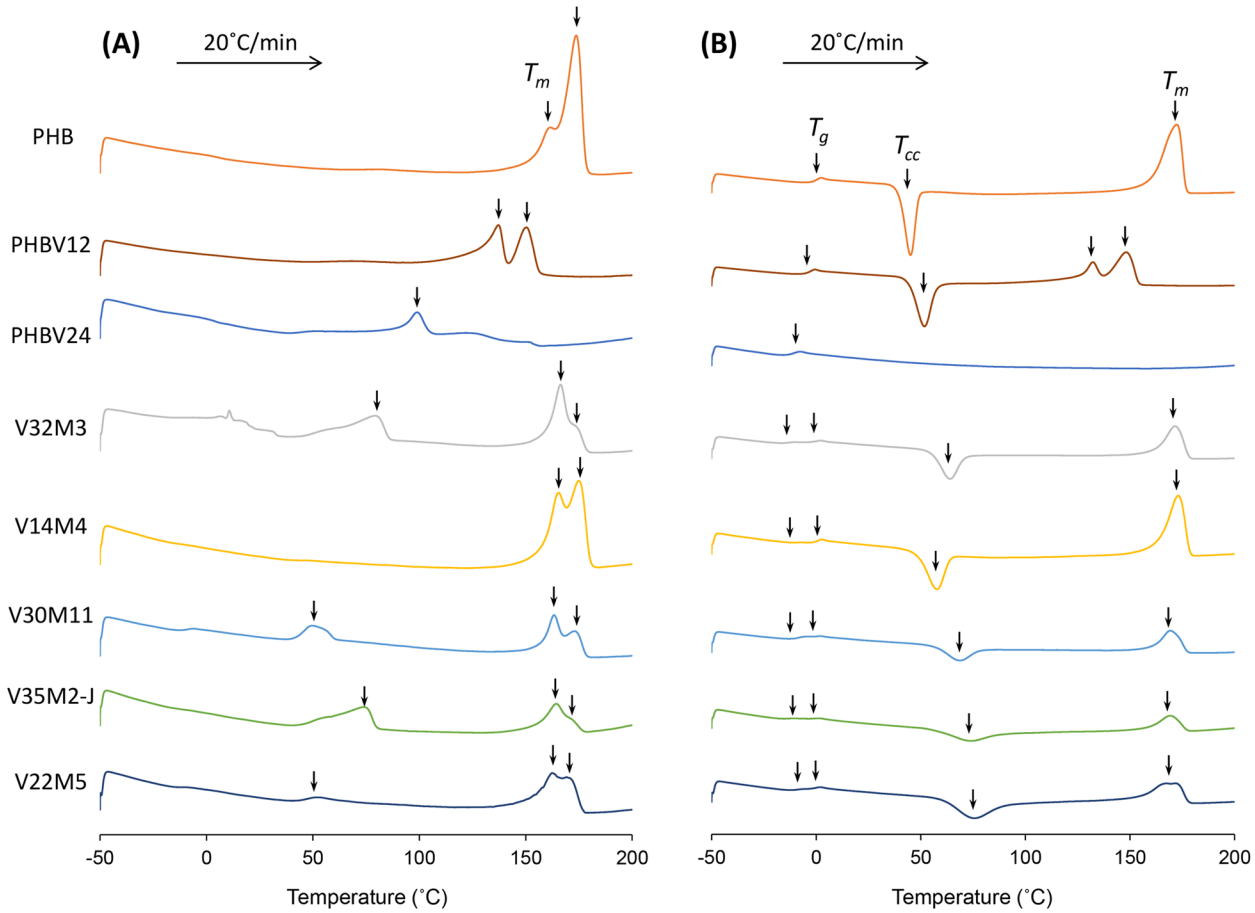

Fig. 7 DSC thermograms of PHB and PHA copolymers. **A** First heating scan, **B** second heating scan

and crystallization behavior of the biosynthesized PHA copolymers were determined and compared with those of PHB, PHBV12, and PHBV24 (Fig. 7, Table 2).

In the first heating scan of DSC, the melting temperatures (T_m) of PHBV12 and PHBV24 were detected at 137–150 °C and 99 °C, respectively. In contrast, α-methylated PHA showed two distinguishable T_ms at 50–80 °C and 162–179 °C. Additionally, the enthalpy of fusion (ΔH_m) of sample V14M4 (containing 14 mol% 3HV and 4 mol% 3H2MV) determined from the first heating scan was 47 J/g, which is much higher than that of PHBV12 (28 J/g). The ΔH_m of V14M4 and PHBV12 diverged despite their 3HV fractions being comparable at 14 mol% and 12 mol%, respectively.

In the DSC second heating scan, the cold crystallization temperatures (T_{cc}) of PHB, PHBV12, and α-methylated PHAs were detected at 45, 51, and 58–75 °C, respectively, whereas that of PHBV24 was not detectable. Although α-methylated PHAs contain 14–35 mol% 3HV, their crystallization behavior is more similar to that of PHB compared to that of PHBV24.

To further investigate the crystallization behavior, crystallization during the cooling process was examined (Fig. 8). The T_c of PHB and V14M4 were 68 °C and 57 °C, respectively. The higher T_c detected during the DSC cooling process indicates that the polymer easily crystallized in the high-temperature range. On the other hand, PHBV12 did not show T_c during the DSC cooling process.

Discussion

PHAs containing α-methylated monomers such as 3H2MB and 3H2MV are a new class of biobased materials with novel properties. Although α-methylated PHA has been marginally detected in activated sludge [27–29], the microorganism and PHA synthase for the biosynthesis of α-methylated PHA have not been isolated, and the metabolic pathways supplying these monomers are yet to be elucidated. Recently, an artificial metabolic

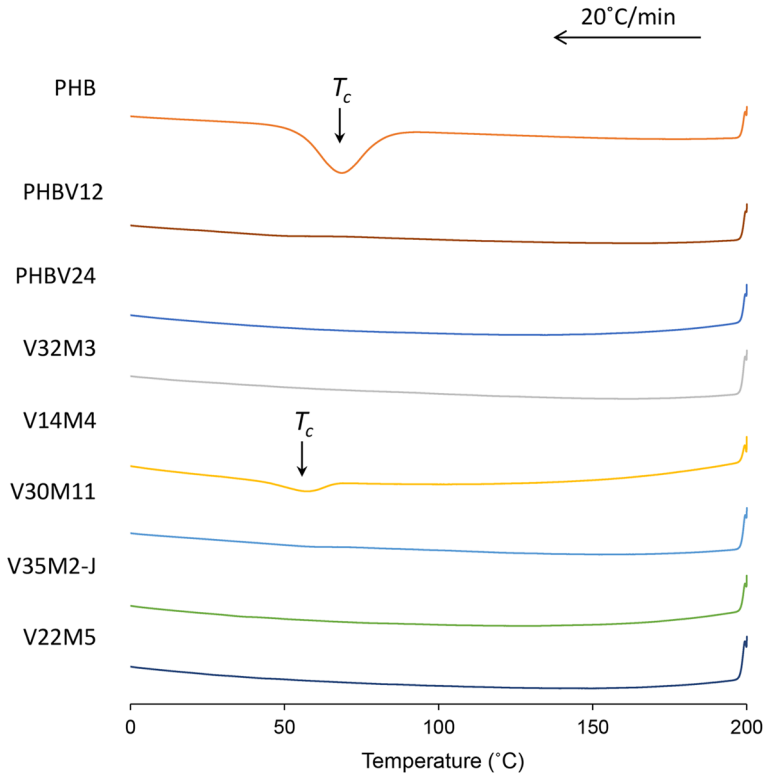

Fig. 8 DSC thermograms during the cooling process of PHB and PHA copolymers

pathway capable of producing the 3H2MB monomer from tiglic acid was constructed by expressing enoyl-CoA hydratase ($PhaJ_{Ac}$) and PHA synthase ($PhaC_{Ac}$–NSDG) with broad substrate specificity in recombinant *E. coli* LSBJ. Therefore, PHA copolymers with a wide range of 3H2MB fractions and P(3H2MB) were biosynthesized [12, 14–17]. Employing the aforementioned artificial metabolic pathway, PHA containing 3H2MV and 3H2MP monomer units, which are methylated at the α-carbon of the 3HV and 3-hydroxypropionate (3HP) monomers, were biosynthesized from *trans*-2-methyl-2-pentenoic acid and the hydrolyzed methyl 3-hydroxy-2-methylpropionate, respectively [18, 19]. Additionally, the novel type of α-methylated PHA with 3-hydroxypyvalic acid, dimethylated at the α-carbon of 3HP, was biosynthesized using sodium 3-hydroxypivalate as a precursor [30]. This approach facilitated the production of various binary PHA copolymers composed of 3HB and α-methylated monomer units. The mechanical and thermal properties of the binary copolymers of α-methylated PHA have been characterized; however, the effects of the α-methylated monomer units in PHA copolymers remain insufficiently explored. Utilizing the Claisen condensation reaction of acetyl-CoA and propionyl-CoA catalyzed by Acat3, a ketothiolase derived from *A. suum*, we successfully biosynthesized a PHA copolymer containing 3HB, 3HV, and α-methylated monomers (3H2MB and 3H2MV) from glucose and propionate [20, 21]. In this study, the biosynthesis of PHA copolymers containing α-methylated monomers was conducted by cultivating the recombinant *E. coli* expressing Acat3. Subsequently, the biosynthesized PHAs were characterized regarding chemical structure and thermal properties.

The biosynthesis of PHA copolymer with 2.4 mol% of α-methylated monomers was achieved by cultivating the recombinant *E. coli* LSBJ expressing Acat3, $PhaC_{Ac}$–NSDG, and $PhaB_{Re}$ from 20 g/L glucose and 9 g/L sodium propionate (Fig. 4). However, the PHA yield was as low as 0.04 g/L due to the toxicity of the added sodium propionate for cell growth. Implementing strategies such as two-stage cultivation consisting of cell growth- and PHA accumulation phases and utilizing strains capable of producing propionate intracellularly may improve PHA production [31]. By the additional expression of $PhaJ_{Ac}$, the composition of α-methylated monomers increased to 15.9 mol% (Fig. 4), suggesting that $PhaJ_{Ac}$ enables to increase the supply of α-methylated monomers, especially 3H2MV.

The stereoregularity of the α-methylated monomers should be considered, due to the isomeric forms derived from the chirality of α- and β-carbon. Given the substrate

specificity of PHA synthase and acetoacetyl-CoA reductase (PhaB), the β-carbon in the α-methylated monomer was presumed to be a (3*R*)-isomer. Meanwhile, it was recently reported that $PhaC_{Ac}$_NSDG polymerizes the (2*S*)-isomer [19]. Differences in the tacticity of the PHA influence its thermal and mechanical properties. Atactic P(3H2MP) (*R*: *S* = 40:60) is amorphous, whereas isotactic P(3H2MP) (*R*: *S* = 1: 99) is crystalline. Moreover, the atactic P(3H2MP) (*R*: *S* = 17: 83) showed elongation at break of 880%, which is two-fold higher compared with isotactic P(3H2MP) (*R*: *S* = 1: 99) [19]. Therefore, controlling the stereoregularity of the α-methylated monomer units is of great interest for further altering the material properties of PHA polymers. In the present study, the chiral configuration analysis showed that the 3H2MV unit in the sample V35M2-J (produced by non-$PhaJ_{Ac}$-expressing strain) contained 42% of (2*R*)- and 58% of (2*S*)-isomers. In contrast, the (2*R*)-isomer ratio was increased in the sample V22M5 (produced by $PhaJ_{Ac}$ expression strain), resulting in up to 79% of (2*R*)-isomer being observed (Fig. 6). A previous study identified the 3H2MB monomer generated via $PhaJ_{Ac}$ from tiglic acid as the (2*R*)-isomer [16]. PHBM11 containing 11 mol% 3H2MV, synthesized in the same manner [18], was also characterized as a (2*R*)-isomer in this study (Fig. 6). From these facts, it is hypothesized that 3-oxo-2-methylvaleryl-CoA generated by Acat3 undergoes dehydration by an inherent enzyme, forming 2-methyl-2-pentenoyl-CoA. Subsequently, $PhaJ_{Ac}$ converts it into (2*R*,3*R*)-3H2MV-CoA stereospecifically (Fig. 3). By heterologously expressing $PhaJ_{Ac}$ and regulating the inherent isomerization in the cells, it may be possible to control the stereoregularity of α-methylated PHA.

In general, for 3HB-based copolymers, 3HB crystallization is inhibited by the presence of co-monomer constituents in the 3HB sequence [6, 9–11]. Interestingly, in this investigation, the 4 mol% 3H2MV-containing copolymer (V14M4), despite having a 14 mol% 3HV fraction, crystallized more readily than PHBV12 during DSC heating and cooling scans (Table 2, Figs. 7 and 8). This result suggests that α-methylated monomers potentially facilitate crystallization. However, to accurately interpret this result, it is necessary to consider that V14M4 is a copolymer with a highly blocky nature (*D* = 13.8). As for sample V30M11, which shows the lowest *D* value (2.19) among the samples synthesized in this study, it exhibited a clear cold crystallization peak at 68 °C during the second DSC heating scan, although PHBV24 did not exhibit a cold crystallization peak (Fig. 7). Comparing these two samples clarified the effect of the 3H2MV unit on the crystallization. This phenomenon might occur due to the promotion of primary nucleation, similar to the behavior observed for PHA polymers containing the 3H2MB unit [15, 16].

Previous studies have reported that PHA polymers with α-methylated monomers, such as 3H2MB and 3H2MV, show superior thermal properties and crystallization behavior [16, 18]. Indeed, for the P(3H2MB), the primary nucleation rate was 200-fold higher than that of PHB [16]. This crystallization behavior is comparable to that of isotactic polypropylene. Additionally, the half-crystallization time of PHBM11 during isothermal crystallization has been reported to be much shorter than that of PHBV12 [11, 18]. Moreover, α-methylated PHA such as P(3H2MB), P(3H2MP), and P(3HPi) exhibit high thermal stability due to their resistance to thermal decomposition, which is induced by the *cis*-elimination, achieved through the substitution of a hydrogen atom at α-carbon with a methyl group [16, 19, 32, 33]. Thus, introducing α-methylated monomers into PHA facilitates crystallization and enhances thermal stability, enabling practical melt processing.

Conclusions

In conclusion, we constructed an artificial metabolic pathway in recombinant *E. coli* LSBJ expressing Acat3 and some PHA biosynthesis enzymes to synthesize a PHA copolymer with α-methylated monomers from glucose and propionate. The biosynthesized PHA copolymer contained up to 15.9 mol% of α-methylated monomers (3H2MV and 3H2MB). The α-carbon of 3H2MV generated by the Acat3-expressing strain was both of (2*S*)- and (2*R*)-isomers, whereas the (2*R*)-isomer was dominant 3H2MV in the strain with additional $PhaJ_{Ac}$ expression. The biosynthesized α-methylated PHA copolymer's thermal properties were evaluated using DSC and compared with the conventional PHAs such as PHB, PHBV12, and PHBV24. The crystallization of α-methylated PHA occurred more rapidly than for PHBV24 because of the incorporation of the 3H2MV monomer. This finding is based on the observation that the T_{cc} of α-methylated PHA was detected during the second DSC heating scan, while PHBV24 was not. This phenomenon occurred due to the promotion of crystal nucleation, which is similar to the behavior observed for P(3H2MB) [16].

Supplementary Information

The online version contains supplementary material available at https://doi.org/10.1186/s44316-024-00008-9.

Supplementary Material 1.

Acknowledgements
The authors thank the Materials Analysis Division, Open Facility Center, Tokyo Institute of Technology, for supporting the NMR measurements.

Authors' contributions
Conceived the project: YM and TT, data collection and analysis: YM and MI, wrote the manuscript: YM, methodology and data curation: YM and MI, reviewed and edited the manuscript: ST, CTN, HA, and TT, funding acquisition: TT. All authors had read and agreed to the published version of the manuscript.

Funding
This study was funded by the JSPS KAKENHI (grant number 21H03640 to T.T.).

Availability of data and materials
No datasets were generated or analysed during the current study.

Declarations

Competing interests
The authors declare no competing interests.

Author details
[1]Department of Materials Science and Engineering, Tokyo Institute of Technology, 4259 Nagatsuta, Midori-ku, Yokohama 226-8502, Japan. [2]Department of Biological Sciences, College of Science, University of Idaho, 875 Perimeter Dr., Moscow, ID 83844-3010, USA. [3]Graduate School of Science, Technology and Innovation, Kobe University, 1-1 Rokkodai-cho, Nada, Kobe 657-8501, Japan. [4]Bioplastic Research Team, RIKEN Center for Sustainable Resource Science, 2-1 Hirosawa, Wako, Saitama 351-0198, Japan.

Received: 10 May 2024 Accepted: 19 June 2024
Published online: 12 August 2024

References

1. Sudesh K, Abe H, Doi Y. Synthesis, structure and properties of polyhydroxyalkanoates: biological polyesters. Prog Polym Sci. 2000;25:1503–55.
2. Chen GQ, Hajnal I, Wu H, Lv L, Ye J. Engineering biosynthesis mechanisms for diversifying polyhydroxyalkanoates. Trends Biotechnol. 2015;33:565–74.
3. Tsuge T. Metabolic improvements and use of inexpensive carbon sources in microbial production of polyhydroxyalkanoates. J Biosci Bioeng. 2002;94:579–84.
4. Suzuki M, Tachibana Y, Kasuya KI. Biodegradability of poly(3-hydroxyalkanoate) and poly(ε-caprolactone) via biological carbon cycles in marine environments. Polym J. 2021;53:47–66.
5. Hachisuka S, Sakurai T, Mizuno S, Kosuge K, Endo S, Ishii-Hyakutake M, Miyahara Y, Yamazaki M, Tsuge T. Isolation and characterization of polyhydroxyalkanoate-degrading bacteria in seawater at two different depths from Suruga Bay. Appl Environ Microb. 2023;89:11.
6. Choi SY, Cho IJ, Lee Y, Kim YJ, Kim KJ, Lee SY. Microbial polyhydroxyalkanoates and nonnatural polyesters. Adv Mater. 2020;32:1907138.
7. Doi Y, Kitamura S, Abe H. Microbial synthesis and characterization of poly(3-hydroxybutyrate-*co*-3-hydroxyhexanoate). Macromolecules. 1995;28:4822–8.
8. Turco R, Santagata G, Corrado I, Pezzella C, Serio MD. *In vivo* and post-synthesis strategies to enhance the properties of PHB-based materials: a review. Front Bioeng Biotechnol. 2021;8:619266.
9. Jonnalagadda D, Kuboki T. Effect of natural flours on crystallization behaviors of poly(3-hydroxybutyrate-*co*-3-hydroxyhexanoate). J Appl Polym Sci. 2016;133:43600.
10. Kai W, He Y, Inoue Y. Fast crystallization of poly(3-hydroxybutyrate) and poly(3-hydroxybutyrate-*co*-3-hydroxyvalerate) with talc and boron nitride as nucleating agents. Polym Int. 2005;54:780–9.
11. Gunaratne LMWK, Shanks RA. Multiple melting behaviour of poly(3-hydroxybutyrate-*co*-hydroxyvalerate) using step-scan DSC. Eur Polym J. 2005;41:2980–8.
12. Watanabe Y, Ishizuka K, Furutate S, Abe H, Tsuge T. Biosynthesis and characterization of novel poly(3-hydroxybutyrate-*co*-3-hydroxy-2-methylbutyrate): thermal behavior associated with α-carbon methylation. RSC Adv. 2015;5:58679.
13. Taguchi S, Yamada M, Matsumoto K, Tajima K, Satoh Y, Munekata M, Ohno K, Kohda K, Shimamura Y, Kambe H, Obata S. A microbial factory for lactate-based polyestersusing a lactate-polymerizing enzyme. Proc Natl Acad Sci USA. 2008;11:17323–7.
14. Furutate S, Nakazaki H, Maejima K, Hiroe A, Abe H, Tsuge T. Biosynthesis and characterization of novel polyhydroxyalkanoate copolymers consisting of 3-hydroxy-2-methylbutyrate and 3-hydroxyhexanoate. J Polym Res. 2017;24:221.
15. Furutate S, Abe H, Tsuge T. Thermal properties of poly(3-hydroxy-2-methylbutyrate-*co*-3-hydroxybutyrate) copolymers with narrow comonomer-unit compositional distributions. Polym J. 2021;53:1451–7.
16. Furutate S, Kamoi J, Nomura CT, Taguchi S, Abe H, Tsuge T. Superior thermal stability and fast crystallization behavior of a novel, biodegradable α-methylated bacterial polyester. NPG Asia Mater. 2021;13:31.
17. Sivashankari RM, Mierzati M, Miyahara Y, Mizuno S, Nomura CT, Taguchi S, Abe H, Tsuge T. Exploring Class I polyhydroxyalkanoate synthases with broad substrate specificity for polymerization of structurally diverse monomer units. Front Bioeng Biotechnol. 2023;11:1114946.
18. Miyahara Y, Nakamura T, Mierzati M, Qie Z, Shibasaka T, Nomura CT, Taguchi S, Abe H, Tsuge T. Thermal and crystallization properties of a polyhydroxyalkanoate binary copolymer containing 3-hydroxybutyrate and 3-hydroxy-2-methylvalerate units. Processes. 2023;11:1901.
19. Mierzati M, Miyahara Y, Curial B, Nomura CT, Taguchi S, Tsuge T. Tacticity characterization of biosynthesized polyhydroxyalkanoates containing (*S*)- and (*R*)-3-hydroxy-2-methylpropionate units. Biomacromol. 2024;25:444–54.
20. Blaisse MR, Dong H, Fu B, Chang MCY. Discovery and engineering of pathways for production of α-branched organic acids. J Am Chem Soc. 2017;139:14526–32.
21. Dong H, Liffland S, Hillmyer MA, Chang MCY. Engineering in vivo production of α-branched polyesters. J Am Chem Soc. 2019;141:16877–83.
22. Tappel CR, Wang Q, Nomura CT. Precise control of repeating unit composition in biodegradable poly(3-hydroxyalkanoate) polymers synthesized by *Escherichia coli*. J Biosci Bioeng. 2012;113:480–6.
23. Tappel RC, Kucharski JM, Mastroianni JM, Stipanovic AJ, Nomura CT. Biosynthesis of poly[(*R*)-3-hydroxyalkanoate] copolymers with controlled repeating unit compositions and physical properties. Biomacromol. 2012;13:2964–72.
24. Miyahara Y, Oota M, Tsuge T. NADPH supply for poly(3-hydroxybutyrate) synthesis concomitant with enzymatic oxidation of phosphite. J Biosci Bioeng. 2018;126:764–8.
25. Miyahara Y, Wang CT, Ishi-Hyakutake M, Tsuge T. Continuous supply of non-combustible gas mixture for safe autotrophic culture to produce polyhydroxyalkanoate by hydrogen-oxidizing bacteria. Bioengineering. 2022;9:586.
26. Kamiya N, Yamamoto Y, Inoue Y, Chujo R, Doi Y. Microstructure of bacterially synthesized poly(3-hydroxybutyrate-*co*-3-hydroxyvalerate). Macromolecules. 1989;22:1676–82.
27. Inoue Y, Sano F, Nakamura K, Yoshie N, Saito Y, Satoh H, Mino T, Matsuo T, Doi Y. Microstructure of copoly(3-hydroxyalkanoates) produced in the anaerobic–aerobic activated sludge process. Polym Int. 1996;39:183–9.
28. Michinaka A, Arou J, Onuki M, Satoh H, Mino T. Analysis of polyhydroxyalkanoate (PHA) synthase gene in activated sludge that produces PHA containing 3-hydroxy-2-methylvalerate. Biotechnol Bioeng. 2007;96:871–80.
29. Dai Y, Lambert L, Yuan Z, Keller J. Characterization of polyhydroxyalkanoate copolymer with controllable four-monomer composition. J Biotechnol. 2008;134:137–45.
30. Mierzati M, Sakurai T, Ishii-Hyakutake M, Miyahara Y, Nomura CT, Taguchi S, Abe H, Tsuge T. Biosynthesis, characterization, and biodegradation of elastomeric polyhydroxyalkanoates consisting of α-dimethylated monomer units. Mater Today Sustain. 2023;24:100577.
31. Lee IY, Kim GJ, Shin YC, Chang HN, Park YH. Production of poly(β-hydroxybutyrate-*co*-β-hydroxyvalerate) by two-stage fed-batch fermentation of *Alcaligenes eutrophus*. J Microbiol Biotechnol. 1995;5:292–6.

32. Zhou L, Zhang Z, Shi C, Scoti M, Barange DK, Gowda RR, Chen EYX. Chemically circular, mechanically tough, and melt-processable polyhydroxyalkanoates. Science. 2023;380:64–9.
33. Zhou Z, LaPointe AM, Shaffer TD, Coates GW. Nature-inspired methylated polyhydroxybutyrates from C1 and C4 feedstocks. Nat Chem. 2023;15:856–61.

Publisher's Note